

AT622 Section 13

Elementary Dielectrics: Interaction with Condensed Matter

The object of this section is to introduce elementary properties of dielectric materials that shape the properties of scattering from homogeneous slabs and particles.

13.1 Polarization of Matter

The *polarization* of matter, in contrast to the polarization of radiation, is a property that relates to the ability of the material to form dipoles. This polarization occurs either by mechanisms that are induced (Fig. 13.1) or when molecules possess a permanent electric dipole moment so that they align themselves with the dipole moment parallel to the applied electric field. As a consequence of either induced or permanent dipoles, a piece of matter placed in an electric field becomes *electrically polarized* and the material polarized in this way is called a *dielectric*.

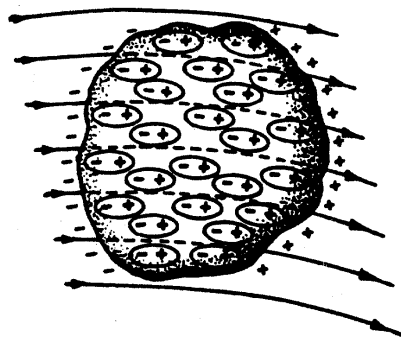


Fig. 13.1 Polarization of matter under the influence of an electric field.

The polarization per unit volume of matter is defined as

$$\vec{P} = (\epsilon_r - 1)\epsilon_0\vec{E} \quad (13.1)$$

where ϵ_0 is the electric permittivity in a vacuum. This macroscopic expression states that the electric field and polarization are directly related and the proportionality constant, ϵ_r , is referred to as the relative permittivity or alternatively as the optical or dielectric constant.

Various mechanisms cause displacement of charge in matter and therefore contribute to its polarizability. Under the influence of oscillatory fields of different frequency, the constituents of matter vibrate on different time scales and thus contribute to the observed properties in different portions of the electromagnetic spectrum. Figure 13.2 schematically depicts the three principal polarization mechanisms that are relevant to atmospheric radiation. Lightest parts (electrons) vibrate fastest (UV)—the heavier parts (atoms and molecules are more sluggish-IR and microwave). One of the mechanisms of interest involves oscillations and the other relaxation.

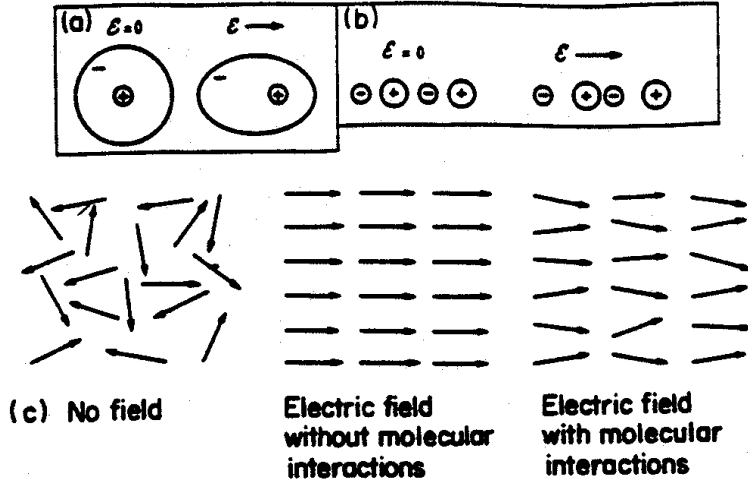


Fig. 13.2 The three main mechanisms of polarization under consideration are (a) electronic (b) atomic, and (c) orientation.

Let us now consider what happens to an individual dipole when an electric field is applied to it. The dipole moment of an individual atom or molecule \vec{p} can be related to the locally active electric field E' by where α is the *polarizability** of the material. If there are N of these molecules per unit volume of matter, then the polarization per unit volume of the material is $\vec{P} = N\vec{p}$.

$$\vec{p} = \alpha \vec{E}' \quad (13.2)$$

We cannot yet combine Eqns. (13.2) and (13.1) to establish the link between the macroscopic parameter ϵ_r to the microscopic parameter α . The problem is that in condensed matter where molecules are tightly packed, the field E' acting locally on the dipole is not the same as the external field E applied to the material. We will not discuss the way that we can express the local field in terms of the applied field here and references elaborating on this topic are given at the end of this chapter. Suffice to say that the field at the dipole may be derived by imagining that it sits in a spherical hole in a surrounding dielectric material. The field in such a hole is increased over a uniform static field E by an amount $P/3\epsilon_0$. The same argument applies for an electric field in the form of a wave so long as the wavelength of the wave is much longer than the spacing between atoms and molecules. In this case, the field locally is increased by the fields associated with the neighboring dipoles such that

$$E' = E + \frac{P}{3\epsilon_0} = \frac{E}{3}(\epsilon_r + 2). \quad (13.3)$$

Combining Eqns. (13.1) and (13.3) produces

$$N\alpha = 3\epsilon_0 \frac{\epsilon_r - 1}{\epsilon_r + 2}, \quad (13.4)$$

*There are different forms of polarizability that can be defined. The polarizability introduced later is referred to as the atomic polarizability, the ratio of P to E defines the volume polarizability (i.e., $N\alpha$) and the quantity $N_o\alpha$ is the molar polarizability where N_o is Avocado's number.

which is known as the *Clausius-Mosotti* equation.

13.2 Classical Theories

The relative permittivity ϵ_r , a property relating the response of dense matter to the action of an electric field, is obviously related to the properties of atoms and molecules of the material as suggested by our discussion of Fig. 13.2. In this section, we provide a more quantitative, albeit phenomenological, account of how this quantity relates to these properties.

Actual calculation of ϵ_r reduces to the calculation of the polarizability of atoms or molecules. This amounts to determining the effects of an external field on the motion of charge in the material following the laws of quantum mechanics. For our purposes, simplified mechanical models suffice to approximate the permittivity.

(a) *The Lorentz Model*

We often picture in our minds a model of an atom represented by electrons whirling around a nucleus in a kind of fuzzy orbit. So far as problems involving nonresonant interaction with radiation, these electrons behave as though they are attached to springs producing a distortion of charge in response to an oscillating electric field. These electrons react to electromagnetic radiation in such a way that they vibrate just like a classical harmonic oscillator (Fig. 13.3). H.A. Lorentz introduced his model of electronic and atomic polarization around the beginning of this century based on the principle of a classical harmonic oscillator.

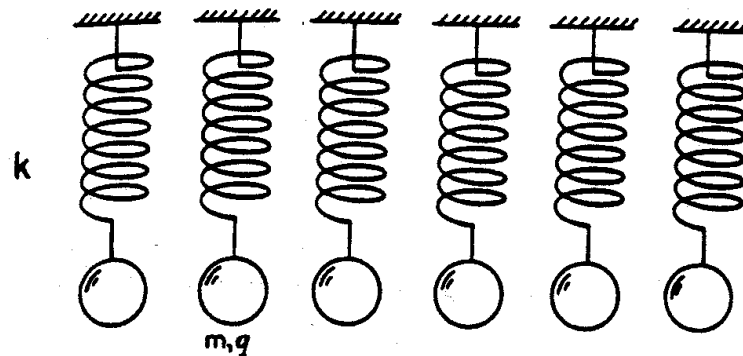


Fig. 13.3 *The Lorentz model of matter.*

The equation of motion of such an oscillator is

$$m \frac{d^2 x}{dt^2} + \gamma \frac{dx}{dt} + kx = qE', \quad (13.5)$$

where m is the mass of the oscillator, $\gamma dx/dt$ is the damping force exerted by neighboring dipoles, and k is the 'spring' constant. In this expression, qE' is the driving force produced by the local electric field E' , and x is the displacement of the mass from its equilibrium position. This is not really a legitimate model of an atom but simple cases of correct quantum mechanical theory gives results equivalent to this model. In a crude sense, the effects of quantum theory are accounted for by the appropriate choice of the properties of oscillators.

If the electric field acting on the dipole vibrates with a frequency ω , the displacement x of the charge oscillates at the same frequency. Assuming that $x = x_0 e^{i\omega t}$, then x can be solved for in terms of E' producing

$$x = \frac{(q/m)E'}{\omega_0^2 - \omega^2 - i\gamma\omega}, \quad (13.6)$$

where $\gamma = b/m$ and $\omega_0 = \sqrt{k/m}$ is referred to as the resonant frequency of the oscillator. This displacement is complex and it is convenient to express it in the form $Ae^{i\Phi}(q/m)E'$ where $A(q/m)E'$ is the amplitude of the oscillation and Φ is its phase relative to the driving force of the electric field. Simple algebra provides us with

$$A = \frac{1}{[(\omega_0^2 - \omega^2)^2 + \gamma^2\omega^2]^{1/2}} \quad (13.7a)$$

$$\Phi = \tan^{-1} \frac{\gamma\omega}{\omega_0^2 - \omega^2} \quad (13.7b)$$

which follow from Eqn. (13.6). An interpretation of these results is provided in Fig. 13.4a and b where A and Φ are shown as a function of frequency ω . How these properties of the oscillator vary with frequency depends on the value of ω relative to the resonant frequency ω_0 of the oscillator. For $\omega \gg \omega_0$, the nonresonant oscillations are weak and out of phase with the driving force of the light. The amplitudes of the oscillation for this range of frequencies, according to Eqn. (13.7a), decreases at a rate proportional to $1/\omega^2$ (Fig. 13.4b). In the spectral range of low frequencies $\omega \ll \omega_0$, the nonresonant oscillations are again weak but, in this case, in phase with the driving force (Fig. 13.4a). In this spectral range, the amplitude approaches a constant value as ω is decreased from resonance. Only the resonance case ($\omega = \omega_0$ and $\Phi = 0$) corresponds to a transition from one quantum state to another.

Given the response of the single oscillator to a time-harmonic electric field, the relative permittivity can be derived using the definition of the dipole moment for a single oscillator as $p = qx$, and since $p = \alpha E'$, then

$$\alpha = \frac{q^2/m}{\omega_0^2 - \omega^2 - i\gamma\omega}$$

and the polarization per unit volume, P for N oscillators in a unit volume follows as

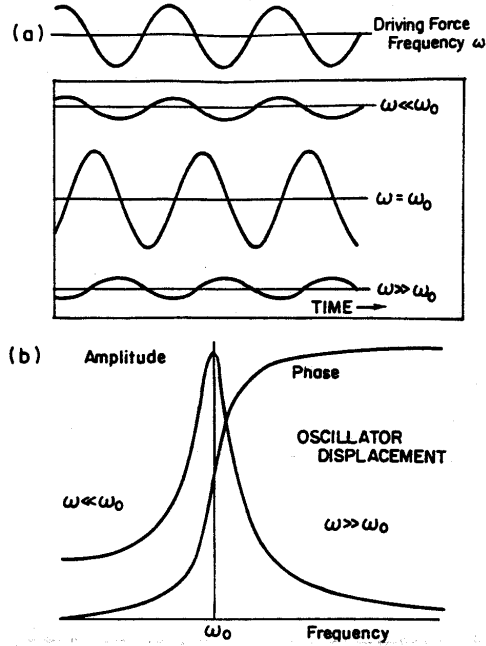


Fig. 13.4 (a) The response of an oscillator to a periodic driving force serves as a model of how charges in matter react to an electromagnetic driving force. The response of the oscillator depends on the frequency of the forcing ω to the oscillator's resonant frequency ω_0 . (b) The oscillator amplitude and phase as a function of the ratio between the frequency ω and the resonant frequency ω_0 . The amplitude approaches a constant value when the frequency of the driving force is much below resonance as in the case of N_2 and O_2 molecules exposed to visible light.

$$P = \frac{\omega_p^2}{\omega_0^2 - \omega^2 - i\gamma\omega} \epsilon_0 E' \quad (13.8)$$

where $\omega_p^2 = Nq^2 / \epsilon_0 m$ is the *plasma frequency*. The difference between the local field and the external field is ignored since a proper treatment of local field effects only complicates matters without adding further insight. With this assumption, it follows by matching Eqn. (13.1) to Eqn. (13.8) that

$$\epsilon_r = 1 + \frac{\omega_p^2}{\omega_0^2 - \omega^2 - i\gamma\omega} \quad (13.9)$$

which has the following real and imaginary parts

$$\epsilon_r' = 1 + \frac{\omega_p^2 (\omega_0^2 - \omega^2)}{(\omega_0^2 - \omega^2)^2 + \gamma^2 \omega^2} \quad (13.10a)$$

$$\epsilon_r'' = \frac{\omega_p^2 \gamma \omega}{(\omega_0^2 - \omega^2)^2 + \gamma^2 \omega^2} \quad (13.10b)$$

respectively. The frequency dependence of each of these components is schematically shown in Fig. 13.5a. The complex component provides the dampening of the oscillations and is a maximum at resonance and coincides with the most rapid change of the real part of the relative permittivity with frequency.

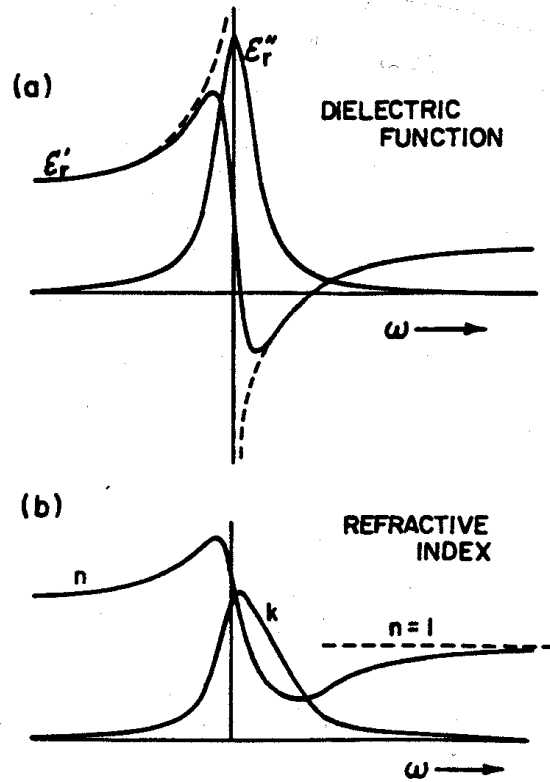


Fig. 13.5 (a) The frequency dependence of the real and complex parts of the relative permittivity. Note that when the damping terms are neglected, $\gamma = 0$ and $\epsilon_r'' = 0$ and the unphysical result occurs at the resonant frequency (dashed curve). Damping is not a result of the viscous movement of the oscillators but represents transitions from one state to another and therefore represents absorption processes. (b) The frequency dependence of the real and complex parts of the refractive index.

Quantum mechanical solutions provide similar results but with the following modifications. Atoms and molecules have several natural frequencies and each has its own dissipation constant. The effective strength of each mode is also different and we represent this by the strength factor f . Summing over all modes leads to a modification of Eqn. (13.9) of the form

$$\epsilon_r - 1 = \frac{Nq^2}{\epsilon_0 m} \sum_i \frac{f_i}{\omega_i^2 - \omega^2 - i\gamma_i \omega} \quad (13.11)$$

(b) *Orientational Polarization-Debye Relaxation*

Lorentz's classical model describes polarization arising from the distortion of charge in nonpolar molecules. In solids and liquids composed of polar molecules, the orientation of the dipoles with respect to an electric field produces an additional low frequency contribution to the polarization. The ability of a molecule to reorient depends on its shape and its interactions with the environment. The nearer to

sphericity and the lower the dipole moment, the more easily and faster the molecule reorients itself in a changing electric field. An asymmetrical molecule like H₂O has several stable orientations and changes direction relatively slowly from one stable orientation to another. The average time between these changes is the relaxation time.

The polarization that results via orientation of dipoles can be computed from methods of statistical mechanics. We consider only very simple aspects of these methods here. Consider a molecule with a permanent dipole moment p_o aligned at some angle θ to the electric field. The potential energy of the dipole is (e.g, Kittel, 1971)

$$U = -p_o E' \cos \theta_o .$$

Statistical mechanics tells us that in a state of equilibrium, the relative number of molecules with a potential energy U is

$$e^{-U/KT}$$

and the number of molecules oriented at an angle θ_o

$$n(\theta_o) = n_o e^{p_o E' \cos \theta_o / KT}$$

where K is Boltzmann's constant and T is temperature. For normal temperatures and E fields, this approximates to

$$n(\theta_o) = n_o \left(1 + \frac{p_o E \cos \theta_o}{KT} \right)$$

where n_o is $N/4\pi$ (we find this by integrating $n(\theta_o)$ over θ_o and this should just be N , the total number of molecules). The net dipole moment per unit volume follows from the integration of the moment $p_o \cos \theta_o$ over solid angle $d\Omega = 2\pi \sin \theta_o d\theta_o$,

$$\bar{P} = 2\pi \int_0^\pi n(\theta_o) p_o \cos \theta_o \sin \theta_o d\theta_o ,$$

resulting in an average dipole moment

$$\bar{P} = \frac{N p_o^2}{3KT} E' \tag{13.12}$$

and by combining Eqns. (13.4) and (13.12) leads to

$$\alpha_o = \frac{p_o^2}{3KT} .$$

Debye (1929) has given an elegant discussion of dielectric relaxation of polar molecules in liquids. He supposed that dipoles initially aligned themselves in the direction of a field only to relax their orientations back to an equilibrium state as defined by the average dipole moment above relevant to a

static field. This relaxation occurs on a time scale τ . The central result of Debye's theory is that the orientational part of the polarizability depends on the applied frequency ω such that

$$\alpha = \frac{p_o^2}{3KT} \frac{1}{1 + i\omega\tau}. \quad (13.13)$$

Using the Mosotti field for E' , then

$$\frac{N\alpha}{3\epsilon_o} = \frac{N}{3\epsilon_o} \left(\frac{p_o^2}{3KT} \frac{1}{1 + i\omega\tau} \right) = \frac{\epsilon_r - 1}{\epsilon_r + 2}. \quad (13.14)$$

From this expression, the complex permittivity is given in terms of the permittivity defined at the limits $\omega \rightarrow 0$ (ϵ_{rs} , the static permittivity) and $\omega \rightarrow \infty$, the high frequency permittivity) and the effective relaxation time constant is,

$$\tau_e = \tau \frac{\epsilon_{rs} + 2}{\epsilon_{rh} + 2},$$

and it follows that

$$\epsilon_r = \epsilon_{rh} + \frac{\epsilon_{rs} - \epsilon_{rh}}{1 + i\omega\tau_e}. \quad (13.15)$$

This expression is the Debye relaxation formula for the permittivity of a friction-dominated medium in which the internal field is assumed to be the Clausius-Mosotti field. The relaxation time is lengthened from τ to τ_e due to the difference between the internal field and the applied field.

The real and imaginary parts of ϵ_r follow from Eqn. (13.15) as

$$\begin{aligned} \epsilon' &= \epsilon_{rh} + \frac{\Delta}{1 + \omega^2 \tau_e^2} \\ \epsilon'' &= \frac{\Delta \omega \tau_e}{1 + \omega^2 \tau_e^2} \end{aligned} \quad (13.16)$$

where $\Delta = \epsilon_{rs} - \epsilon_{rh}$. The imaginary part of the dielectric function, according to Eqn. (13.16), is a maximum at $\omega = 1/\tau_e$, and its behavior with frequency is broadly similar to ϵ_r'' predicted for the Lorentz oscillator. The real part behaves quite differently: it has no maxima or minima but decreases monotonically with increasing frequency from a value of ϵ_{rs} at low frequencies to ϵ_{rh} at high frequencies. At low frequencies, permanent dipoles react to the more slowly oscillating electric field in enough time that they become aligned, producing a significant polarization and large values of ϵ' . At higher frequencies, this part of the matter is unable to respond quickly enough to produce any polarization.

The Debye relaxation model has been successfully used to describe measured values of the dielectric function at microwave frequencies as demonstrated in Fig. 13.6a. Both the real and complex parts of ϵ_r for water at microwave frequencies are compared to the Debye theory on this diagram. The parameters ϵ_{rs} , ϵ_{rh} , and τ are chosen to provide the best fit to the data. An especially relevant consequence of the

relaxation spectrum of H₂O to remote sensing lies in the change of the spectrum of ϵ_r with the phase transition from liquid to solid water. To understand the differences in ϵ_r as this transition occurs it is helpful to consider the simple classical expression Debye derived for τ , namely

$$\tau = \frac{4\pi\eta a^3}{KT}, \quad (13.17)$$

for a sphere of radius a in a fluid of viscosity η . This time constant is a ratio of the viscous-restoring torque applied to the sphere that maintains alignment to the thermal forces that act to disrupt this alignment. When numerical values are substituted into Eqn. (13.17), the derived relaxation time corresponds approximately to that estimated from measurement. A naive interpretation of the phase transition from liquid water to ice is to consider a large discontinuous increase in viscosity that occurs when water freezes. Thus, the permanent electric dipoles that were free to rotate in the liquid are now immobilized. The relaxation time for ice is significantly larger than it is for water leading to smaller values of ϵ_r'' and a dramatic shift in the maximum of ϵ_r' to smaller frequencies. The consequences of such large changes in ϵ_r as ice melts are observed when microwave radiation transmitted by a radar system is backscattered by melting ice particles producing the "bright band" in vertical profiles of radar reflectivity.

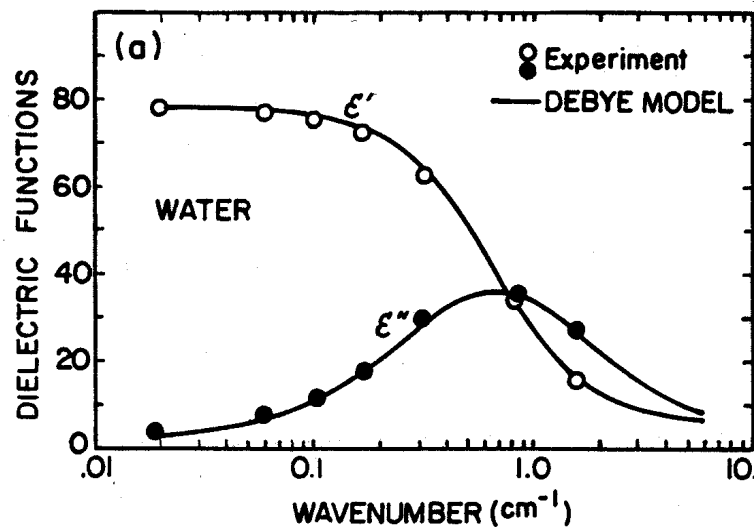


Fig. 13.6 The dielectric function of water at room temperature calculated from the Debye relaxation model with $\tau = 0.8 \times 10^{-11}$ sec, $\epsilon_{rs} = 77.5$, $\epsilon_{rh} = 5.27$. Data were obtained from three sources (after Bohren and Huffman 1993).

(c) Summary

We learn from both models that when a sinusoidal electric field acts on a dielectric material, there is an induced dipole moment that is proportional to the electric field. The proportionality constant $\epsilon_r - 1$ depends on the frequency of the oscillating field and is a complex number, which means that the polarization does not follow the electric field but is shifted in phase. A schematic diagram summarizing the frequency dependence of ϵ_r' and ϵ_r'' for an ideal nonconducting substance is shown in Fig. 13.7. At the low frequency end, ϵ_r' is composed of contributions by all three mechanisms with the largest contributions resulting from dipole orientation processes. As the frequency increases, the dipoles are

unable to respond fast enough, and this mechanism ceases to contribute to ϵ'_r , instead the atomic polarization processes that produce vibrational motions contribute. For the water molecule, the resonances associated with these processes are found at infrared wavelengths. At even higher frequencies, inter-atomic vibrations cannot respond fast enough to the applied field. At these frequencies, the electronic oscillations that are induced by the electric field now contribute to ϵ'_r and the resonant frequencies associated with these oscillators are typically found at UV wavelengths. Finally, as the frequency increases beyond the point where all electronic modes are exhausted, ϵ'_r approaches unity.

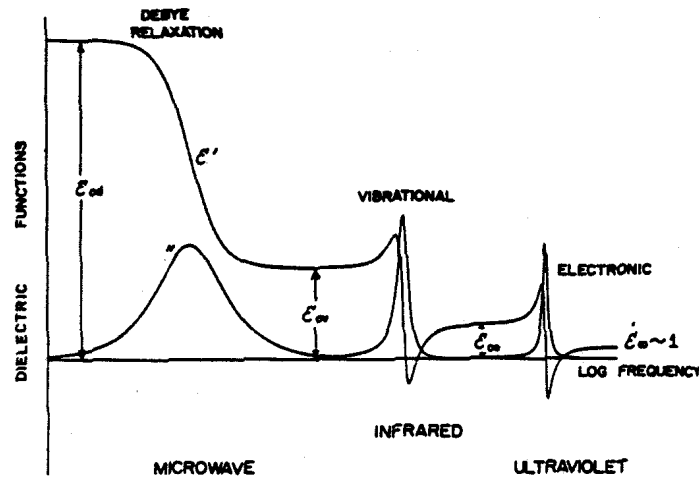


Fig. 13.7 Schematic diagram of the frequency variation of the dielectric function of an ideal nonconductor (Bohren and Huffman, 1983).

Where ϵ'_r changes most dramatically with frequency there is an associated peak in ϵ''_r , which characterizes the absorption of radiation by the substance. This absorption arises from the resonances associated with the vibrations of atoms and molecules of matter. In dense matter, the molecules are so tightly packed together that significant interactions exist between them. The internal modes of the oscillations are therefore modified and the natural frequencies of the atomic oscillations are spread out by the interactions producing a broadening of the absorption lines much in the same way as pressure broadening occurs in gases. In place of the precisely defined characteristic energy levels associated, for example, with the vibration and rotation states of the individual molecules, are energy bands composed of a continuum of levels. Thus the energy levels of the vibration and rotation states of, for instance, a water molecule form a continuous absorption band resulting in a broad absorption spectrum as indicated in Fig. 13.7. Figure 13.8 provides a schematic illustration of the electron energy bands of two different types of material.

Since the energy bands in a solid form as a superposition of the energy levels of the individual molecules, the spectral positions of the more continuous absorption bands for solid matter more or less overlap the absorption spectrum of the individual molecules. Thus the infrared absorption spectra of liquid water and solid ice, for instance, occur at roughly the same wavelengths where absorption bands of water vapor lines are found.

There are features of the energy bands which have a significant bearing on the way radiation interacts with condensed matter and which are therefore important to our understanding of particle scattering. The energy bands of certain materials overlap, as depicted in Fig 4.8, and the electrons in such a material have

a continuous distribution of energy within these overlapped bands. If one of the overlapping bands is partially empty, application of an electric field readily excites electrons into adjacent unoccupied states and an electric current results. The material is said to be a good conductor of electricity and its electrical behavior is determined by both the energy band structure and how the bands are normally filled by electrons. This is the case for metals that can absorb radiation at any wavelength. When a photon is absorbed in a metal, the electron jumps to an excited state. A photon of the same energy is immediately re-emitted and the electron returns to its original state. Because of this rapid and efficient reradiation, the surface of the metal appears reflective rather than absorbant. Another type of material is the nonconductor, which possesses energy bands that are separated by intervals referred to as *forbidden bands*; absorption of radiation by such material is therefore only likely for photons possessing energies greater than this energy gap.

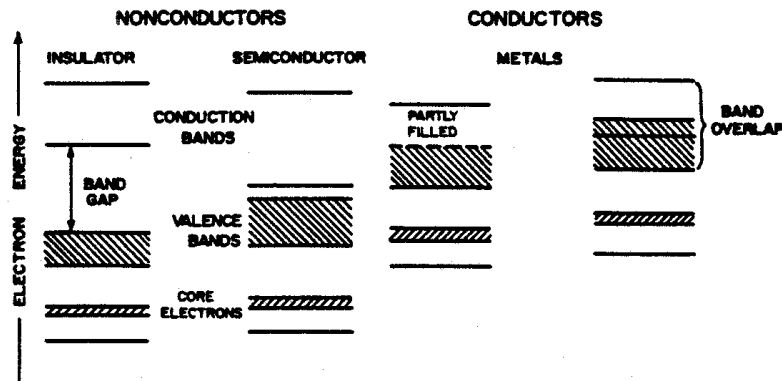


Fig. 13.8 Electron energy bands in nonconductors and conductors. The filled bands are shown hatched (Bohren and Huffman 1983).

13.3 The Refractive Index

The two sets of quantities that are often used to describe optical properties of matter are the relative permittivity ϵ_r and the refractive index m^\dagger . Both are related according to

$$\begin{aligned} \epsilon_r' &= n^2 - \kappa^2 \\ \epsilon_r'' &= 2n\kappa \end{aligned} \tag{13.18}$$

where n and κ are used here to denote the real and imaginary parts of the refractive index, respectively. The spectral variations of both n and κ from the near infrared to the microwave regions are depicted in Fig. 13.9. Certain features of the hypothetical spectra of ϵ_r' and ϵ_r'' shown in Fig. 13.7 can be identified in the refractive index spectra. Readily apparent are the relaxation spectra extending from about the millimeter wavelength range into the centimeter range. For water and ice, the values of κ lead to significant absorptions in clouds when wavelengths are greater than about about 1 μm . For ice, κ decreases again beyond wavelengths of about 100 μm . At microwave frequencies, ice particles in the atmosphere are more effective scatterers of radiation than absorbers, whereas the reverse is true of water drops. There are also significant differences between values of κ for water and ice in the near infrared

[†] The refractive index is sometimes written as $m = n + i\kappa$ and other times as $m = n - i\kappa$. The latter applies when the time dependence of factor of the wave is $\exp(i\omega t)$ rather than $\exp(-i\omega t)$. Both will be used in these notes.

especially around 1.6 and 3.7 μm , which also happen to be channels associated with radiometers flown (or to be flown) on meteorological satellites. The consequence of the different values of n to the transfer of solar radiation through clouds at these wavelengths has been proposed as a way discriminating ice clouds from water clouds.

Determining the refractive indices of atmospheric aerosol is quite a complex problem and a topic of apparent controversy. In Fig. 13.10, the spectra of the imaginary parts of the refractive index of several materials that exist in atmospheric particles are shown. Results are given for water, ammonium sulfate, crystalline quartz, sulfuric acid, carbon, sodium chloride, and hematite over selected spectral regions. As we have come to expect from our previous discussions, κ is large (around unity) in the infrared and ultraviolet spectral regions and small at visible wavelengths for all materials except for carbon and hematite both of which significantly absorb visible light. To emphasize the transparency of the material in the visible region, the dashed line is the value of κ corresponding to a 1% transmission through a 1 cm thick homogeneous slab of material. Only carbon, which has metal like overlapping electronic energy bands (e.g., Fig. 13.8), has high values of κ throughout most of the spectrum. The mineral hematite, although a very minor constituent of the atmospheric aerosol, is one of the few known materials that are also highly absorbing at visible wavelengths.

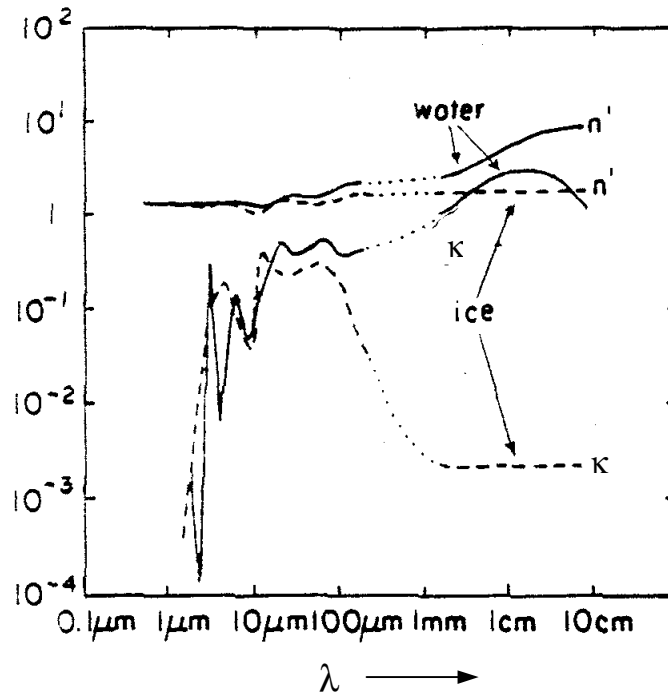


Fig. 13.9 Typical values of the refractive indices for water and ice.

The hatched region in Fig. 13.10 shows the values of κ obtained from remote measurements using a retrieval scheme based on the particle scattering theories discussed in the following chapter. Clearly these derived values of κ do not seem to match those of any of the pure materials that make up the particle, and are presumably some kind of average of a mixture containing a small amount of a highly absorbing material. The meaning of such an average value and its direct application to theories of particle scattering must be treated with caution. Measurement of the refractive index of a substance in a pure homogeneous slab form is difficult enough, and these results highlight the complexity of estimating the refractive index when such material is broken up into small particles of heterogeneous material.

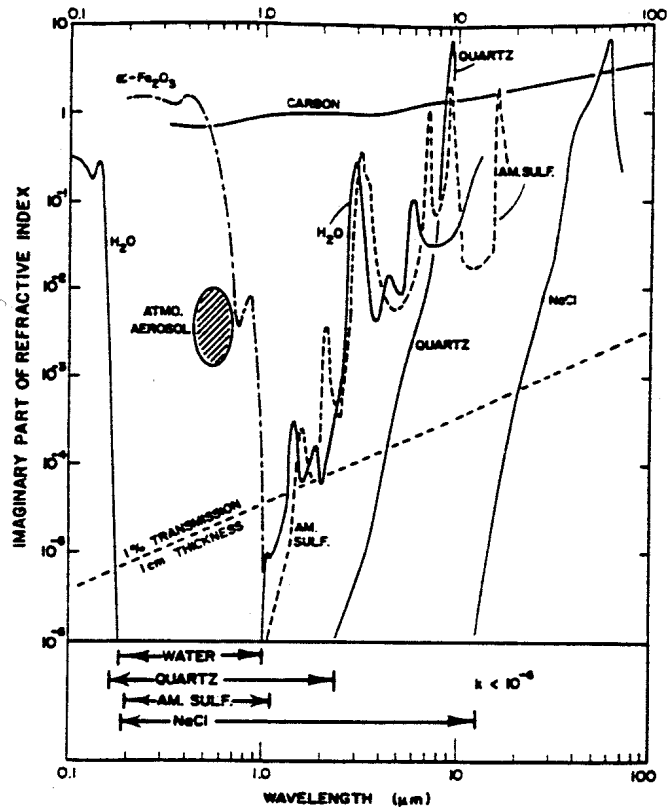


Fig. 13.10 The imaginary part of the refractive index of several solids and liquids that are found as atmospheric particles (Bohren and Huffman, 1983).

13.4 Dielectric Slab

The formal analogy between scattering by a particle and by a slab is shown in Fig. 13.11 in its most general aspect. The wave scattered by a particle is analogous to the waves reflected and transmitted by a slab. However, there are important differences between these two cases that need to be noted. We will learn that particles scatter in complicated ways depending on the direction of scatter whereas the scattering by a slab occurs through the interference effects such that radiation is concentrated only two directions.

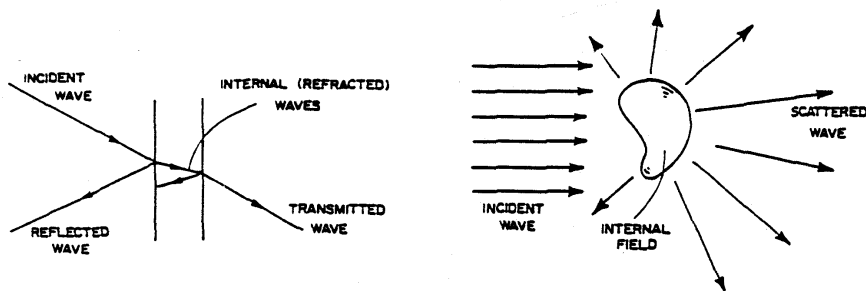


Fig. 13.11 A schematic depicting the analogy between scattering by a slab and by a particle. The scattered wave by a particle is analogous to the wave transmitted and reflected by the slab (from Bohren and Huffman, 1983).

General expression for a propagating plane wave along the z axis is

$$E = E_o e^{i(kz - \omega t)} \quad (13.19)$$

where, in a slab of condensed matter of refractive index m ,

$$kz = mk_o z \quad (13.20)$$

which is defined relative to the wavenumber k_o in a vacuum. In an absorbing slab, m is complex and thus k is complex. For the simplest case of plane wave propagation along the z direction, and with $m = n + i$ in Eqn. (13.20), Eqn. (13.19) may be written as

$$E = E_o \left[e^{-2\pi k / \lambda_o} \right] e^{i(nk_o z - \omega t)}. \quad (13.21)$$

The first of the exponential factors describes the rate at which the radiation is attenuated in the slab. The second exponential factor represents the oscillatory part of the wave and we observe that the real part of the refractive index determines the phase speed of the wave. The attenuation factor can be written in terms of a bulk absorption coefficient $\beta = 4\pi k / \lambda_o$ such that the intensity of the radiation is attenuated according to the formula

$$I = Ie^{-\beta z}. \quad (13.22)$$

A useful and convenient way of interpreting this attenuation is in terms of the penetration depth $d_I = 1/\beta$, which is the depth to which the intensity is reduced by $1/e$ of its incident value.

Example 13.1: Depth of Penetration

Water and ice possess refractive indices that are strongly frequency dependent and thus have a penetration depth that varies significantly from wavelength to wavelength. Calculate the depth of penetration d_I in a water and ice slab for the following wavelengths and refractive indices. What inferences would you make about scattering versus absorption processes by water and ice particles at each wavelength?

Wavelength	Instrument	Refractive Index (n, κ)	
		water	ice
0.7 μm	AVHRR	(1.33, 0)	(1.31, 0)
1.6 μm	AVHRR	(1.317, 8×10^{-5})	(1.31, 0.0003)
3.7 μm	AVHRR	(1.374, 0.0036)	(1.40, 0.0092)
10.8 μm	AVHRR	(1.17, 0.086)	(1.087, 0.182)
0.8 cm	k-band radar	(8.18, 1.96)	(1.789, 0.0094)
10 cm	S-band radar	(5.55, 2.85)	(1.788, 0.00038)

The depths of penetration are listed on the table. From these we can make a number of inferences about the difference between water and ice scattering at the wavelengths given. For example we expect that water surfaces and clouds will be relatively dark (relative to ice surfaces and clouds) at 3.7 μm , that ice particles are relatively transparent at 0.8 cm and more so at 10 cm, and that 1.6 μm may be useful in discriminating ice properties in clouds from water properties (glaciated clouds will be darker, all things equal, than water clouds).